

1 **Technical Note: The impact of spatial scale in bias correction of climate model output for**
2 **hydrologic impact studies**

3 E.P. Maurer¹, D.L. Ficklin², W. Wang³

4 ¹Santa Clara University, Civil Engineering Department, Santa Clara, California, 95053-0563
5 USA, emaurer@engr.scu.edu

6 ²Indiana University, Department of Geography, Bloomington, IN, 47405, USA

7 ³California State University at Monterey Bay, Department of Science and Environmental Policy
8 and NASA Ames Research Center, Moffett Field, CA 94035, USA

9

10 **Abstract**

11 Statistical downscaling is a commonly used technique for translating large-scale climate model
12 output to a scale appropriate for assessing impacts. To ensure downscaled meteorology can be
13 used in climate impact studies, downscaling must correct biases in the large-scale signal. A
14 simple and generally effective method for accommodating systematic biases in large-scale model
15 output is quantile mapping, which has been applied to many variables and shown to reduce
16 biases on average, even in the presence of non-stationarity. Quantile mapping bias correction has
17 been applied at spatial scales ranging from areas of hundreds of kilometers to individual points,
18 such as weather station locations. Since water resources and other models used to simulate
19 climate impacts are sensitive to biases in input meteorology, there is a motivation to apply bias
20 correction at a scale fine enough that the downscaled data closely resembles historically
21 observed data, though past work has identified undesirable consequences to applying quantile
22 mapping at too fine a scale. This study explores the role of the spatial scale at which the quantile-
23 mapping bias correction is applied, in the context of estimating high and low daily streamflows
24 across the Western United States. We vary the spatial scale at which quantile mapping bias
25 correction is performed from 2° (~200 km) to $1/8^\circ$ (~12 km) within a statistical downscaling
26 procedure, and use the downscaled daily precipitation and temperature to drive a hydrology
27 model. We find that little additional benefit is obtained, and some skill is degraded, when using
28 quantile mapping at scales finer than approximately 0.5° (~50 km). This can provide guidance to
29 those applying the quantile mapping bias correction method for hydrologic impacts analysis.

30 **1 Introduction**

31 Climate modeling is an imperfect science, with uncertainties in simulated land surface climate
32 that vary in space and with the forecast time horizon (Hawkins and Sutton, 2009, 2011). This
33 presents a challenge when projecting climate change impacts at a local and regional scale. The
34 most recent coordinated global climate model (GCM) experiments conducted as part of the fifth
35 Coupled Model Intercomparison Project (CMIP5, Taylor et al., 2012) have been used to
36 simulate historic and future climate. These CMIP5 runs have demonstrated improvements over
37 earlier generations of models, both in the representation of physical processes and the simulated
38 fields (Flato et al., 2013; Watterson et al., 2014). While improved skill over the United States has
39 been found for both mean and variability of climate (Sheffield et al., 2013a; Sheffield et al.,
40 2013b), biases remain that must be accommodated for projecting future impacts, for example, on
41 streamflow characteristics (Wood et al., 2004).

42 In this study we focus on a common method used for bias correction, namely quantile mapping.
43 Quantile mapping is effective at removing some climate model biases, is relatively simple to
44 apply, and has been incorporated into many statistical downscaling schemes used for local and
45 regional impacts analysis (Li et al., 2010; Maraun et al., 2010; Panofsky and Brier, 1968; Piani et
46 al., 2010; Themeßl et al., 2011). While quantile mapping bias correction does inherently assume
47 that the biases exhibited by a climate model remain constant in future projections, there is some
48 indication that this is not an unreasonable assumption (Maraun, 2012; Maurer et al., 2013),
49 especially where biases are driven by persistent climate model characteristics, such as inadequate
50 representation of topography. Other discrepancies between historic climate model simulations
51 and observations, especially due to internal natural variability (for example, El Niño events

52 simulated by a freely evolving GCM not coinciding with observations), are not necessarily
53 model biases (Eden et al., 2012), but are corrected nonetheless by quantile mapping, which is
54 blind to the source of the bias. For this reason, the training (or calibration) period for the bias
55 correction should be long enough (typically 10-30 years) so that internal variability is not a
56 dominant source of bias between the climate model and observations.

57 In statistical downscaling approaches that incorporate a quantile mapping bias correction, large-
58 scale climate model output is typically first interpolated onto a regular grid and then bias
59 corrected using quantile mapping with a gridded observational data set at the same spatial
60 resolution (Maurer et al., 2010b;Thrasher et al., 2012). This was originally developed as a
61 method of convenience to place the climate models, which operate natively at many different
62 spatial resolutions, onto a single grid to enable straightforward intercomparisons. Using a
63 common grid for all climate models also ensures that the bias corrected output from each
64 (regridded) climate model, for the time period on which the quantile mapping is calibrated, is
65 statistically identical.

66 The scale at which global climate models were bias corrected for the archive of downscaled
67 climate model output (from the prior CMIP3 experiment (Meehl et al., 2007)), described by
68 Maurer et al. (2007) for the conterminous United States was 2° (latitude and longitude), or
69 roughly 200 km, approximately corresponding to the finest spatial resolution of the participating
70 climate models. Using similar logic, for the expansion of the archive with downscaled CMIP5
71 climate model output (Maurer et al., 2014), which included climate models operating at higher
72 spatial resolutions, the resolution at which bias correction was performed was refined to 1°. Of
73 course, when further spatial disaggregation to finer scale is performed after the bias correction,

74 the correspondence between bias corrected climate model output and observations at the fine
75 scale degrades, since fine-scale climate information is not incorporated in the bias correction.

76 To ensure closer correspondence between the final downscaled product and observations, a
77 temptation is to apply quantile mapping bias correction at a finer scale, which in its limit would
78 be applied at the scale of observations (either at the original grid scale, or even to point
79 observation stations). This approach has been applied to climate model output at many spatial
80 scales: for example, Wood et al. (2004) applied it at a 2° (~200 km) spatial scale; Li et al. (2010)
81 used quantile mapping at 1° (~100 km); Hwang and Graham (2013) and Tian et al. (2014)
82 applied it at $1/8^\circ$ (~12 km); Abatzoglou and Brown (2012) applied quantile mapping at $1/12^\circ$ (~8
83 km); Tryhorn and DeGaetano (2011) used quantile mapping to bias correct to point observations
84 of precipitation and temperature.

85 One problem with applying quantile mapping at fine scales has been identified by Maraun
86 (2013;2014). In summary, the adjustment by quantile mapping inappropriately applies a
87 deterministic variance correction, implicitly assuming that any unexplained variance at the fine
88 spatial scale can be accommodated by rescaling the variance from the large scale. In other words,
89 a climate model grid scale precipitation value (representing average precipitation over
90 approximately $10,000 \text{ km}^2$) would be used to adjust the precipitation (probability distribution) at
91 a much smaller scale (for example, 100 km^2). In essence, this assumes the unexplained
92 variability of fine scale precipitation can be described with a deterministic function of large scale
93 precipitation variability. Since variability at the coarse-scale (due to synoptic circulation, for
94 example) and fine-scale (due to local topographic features, land-atmosphere interactions, etc.)
95 have distinct sources, application of quantile mapping to simultaneously include spatial

96 downscaling is arguably inappropriate. For example, Maraun (2013) highlights an example
97 where a high large-scale precipitation value is translated by quantile mapping to high values at
98 all points within the large-scale grid box, producing an erroneously large and uniform extent of
99 an extreme event; fine-scale variability among the points is not replicated by the deterministic
100 transformation of quantile mapping. It should be noted that where downscaling to point
101 observations is required, others have proposed alternative approaches that expand beyond the
102 quantile mapping used in this study (e.g., Haerter et al., 2015).

103 Another issue with fine-scale application of quantile mapping of precipitation has been related to
104 spatial correlation of storm events (Bárdossy and Pegram, 2012). They found quantile mapping
105 bias correction of precipitation at 25 km decreased spatial correlation with observations, and
106 hence underestimated areal precipitation at larger scales. This could have potential negative
107 effects on flood estimates for large river basins, and Bárdossy and Pegram (2012) propose a
108 recorrelation technique to restore some of the observed spatial structure of precipitation events.
109 A further consideration, when applying quantile mapping to future precipitation projections, is
110 that the relationship between the spatial scale of fine- and coarse-scale precipitation may change
111 in ways that could affect extreme runoff projections (Li et al., 2015).

112 In addition to those noted above, there are other known shortcomings of quantile mapping, some
113 of which have been accommodated by modifying or augmenting quantile mapping or by
114 developing alternative statistical procedures. For example, where it is desired to maintain a joint
115 distribution of multiple variables through bias correction, as opposed to individual variable
116 downscaling as used here, joint downscaling methods have been developed (Abatzoglou and
117 Brown, 2012; Mehrotra and Sharma, 2015; Zhang and Georgakakos, 2012). The probability

118 transformations in quantile mapping are incapable of correcting for GCM biases in low
119 frequency variability, and autoregressive and spectral transformations have been developed to
120 accommodate these biases where important (Mehrotra and Sharma, 2012;Pierce et al., 2015).
121 While we recognize the deficiencies in quantile mapping, as discussed for statistical bias
122 correction in general by Ehret et al. (2012), and there is the promise of recent advances in bias
123 correction, it remains that quantile mapping is widely used and generally effective at removing
124 biases (Gudmundsson et al., 2012), even in the presence of some non-stationarity (Lafon et al.,
125 2012;Maurer et al., 2013;Teutschbein and Seibert, 2013). Our aim in this study is not to advocate
126 for a specific downscaling method, but to understand a specific aspect of this widely used
127 method.

128 The question we aim to address in this study is whether there is a practical limit to spatial scale
129 that should be considered when applying quantile mapping bias correction in statistical
130 downscaling in the context of projecting hydrologic impacts. Past work on Western United States
131 hydrology has found negligible predictive skill, and in some locations a degradation, when bias
132 correction is performed at a fine spatial scale (Maurer et al., 2010b).

133 To assess this, we begin with large-scale climate data (approximately 200 km spatial scale) and
134 perform a quantile mapping bias correction at a variety of spatial scales, as part of a statistical
135 downscaling approach, to obtain fine scale gridded daily precipitation and temperature values.
136 These downscaled meteorological data are used to drive a hydrological model over the Western
137 United States to simulate streamflow at sites where streamflow is observed, representing
138 drainage areas from approximately 100 km² to 600,000 km². Skill is assessed by comparing the
139 streamflow simulated by the downscaled meteorology and the streamflow from a simulation

140 using observed meteorology. Ultimately, we aim to determine whether the improved
141 correspondence between downscaled large-scale climate and fine scale observed meteorology
142 comes with a cost of degraded skill outside of the training period used for bias correction. This
143 can be helpful for guiding future downscaling efforts for assessing the impacts of climate change
144 on water resources.

145 **2 Data and Methods**

146 The quantile mapping bias correction is performed as a first step in the Bias Correction-Spatial
147 Disaggregation (BCSD; Wood et al., 2004) technique. A schematic of the procedure is shown in
148 Figure 1. Observations of gridded daily precipitation and temperature (Livneh et al., 2013) are
149 available at a $1/16^\circ$ spatial resolution; to reduce the computational load they are aggregated to a
150 $1/8^\circ$ (0.125°) resolution for this experiment. The Livneh et al. data use approximately 20,000
151 sites with daily meteorological records to define their field. These $1/8^\circ$ gridded observations are
152 then aggregated to different spatial resolutions to match the interpolated large-scale daily data
153 (X° in Figure 1).

154 A quantile mapping approach is used to bias-correct the large-scale data, in which empirical
155 cumulative distribution functions (CDFs) are developed for both the aggregated observations and
156 the interpolated large-scale data for a calibration period. The quantile for each large-scale value
157 is then determined using its CDF, and the value is transformed to the observed value at the same
158 quantile. This transfer function, following Li et al. (2010), can be written as:

$$x_{\text{model-adjusted}} = F_{\text{obs}}^{-1}(F_{\text{model}}(x_{\text{model}})) \quad (1)$$

159 where F is the CDF for the calibration period, x is a daily value of precipitation or temperature,
160 with the CDF, at each X° grid cell, developed for a moving window of ± 15 days from the day
161 pertaining to x . The subscripts indicate large-scale model data or observations (obs). After the
162 quantile mapping bias correction, precipitation and temperature values are expressed as
163 anomalies relative to the climatological mean for the moving window, using a difference for
164 temperature and a fraction for precipitation. These anomalies are interpolated from the large
165 scale to the final $1/8^\circ$ grid and applied to climatological values to obtain final daily downscaled
166 data. Details of the quantile mapping and BCSD method as applied here are available elsewhere
167 (Maurer et al., 2010b;Thrasher et al., 2012).

168 The large scale climate data we use are daily precipitation and maximum and minimum surface
169 air temperature from the National Centers for Environmental Prediction and the National Center
170 of Atmospheric Research (NCEP/NCAR) reanalysis (Kalnay et al., 1996) as a surrogate for a
171 GCM. Because NCEP/NCAR reanalysis ingests some atmospheric observations (though,
172 importantly, not precipitation) in its production, it exhibits a higher skill than possible with
173 GCMs (Reichler and Kim, 2008). While it arguably represents a best possible simulation
174 capability of a GCM, it still can exhibit substantial regional biases, especially in precipitation
175 (Maurer et al., 2001;Widmann and Bretherton, 2000;Wilby et al., 2000). The assimilation of
176 some observed atmospheric states means that NCEP/NCAR reanalysis can be expected to have
177 some correspondence to observed events, which would be impossible with a freely-evolving
178 GCM. These characteristics make the use of reanalysis data for evaluating bias correction and
179 downscaling procedures common practice (e.g., Huth, 2002;Schmidli et al., 2006;Vrac et al.,
180 2007).

181 Reanalysis data are available on a T62 Gaussian grid (approximately 1.9° square), a resolution
182 comparable to current GCMs. Daily reanalysis precipitation, maximum and minimum
183 temperature are bilinearly interpolated onto regular grids of varying spatial resolutions
184 (designated as X in Figure 1) prior to bias correction: 2.0° , 1.0° , 0.5° , 0.25° , 0.125° . The gridded
185 observations are aggregated to the same spatial scale as the interpolated reanalysis data and the
186 bias correction is then performed at that scale. The period 1960-1989 is used to calibrate or 'train'
187 the bias correction, and 1990-2011 is used to validate the downscaled data. This analysis was
188 conducted over the conterminous United States for all of the spatial resolutions except the 0.125°
189 experiment, which used a smaller domain over the western U.S. for computational reasons.

190 Both the downscaled meteorology and the gridded observations were used to drive three Soil
191 Water and Assessment Tool (SWAT; Arnold et al., 1998) hydrologic models over the western
192 United States (for the Columbia River Basin, Sierra Nevada, and Upper Colorado River Basin).
193 SWAT simulates the entire hydrologic cycle, including surface runoff, snowmelt, lateral soil
194 flow, evapotranspiration, infiltration, deep percolation, and groundwater return flows, at the
195 subbasin scale. The subbasins delineated for these SWAT models have average areas ranging
196 from 246 km^2 (for the Colorado basin) to 191 km^2 (for the Sierra), comparable to that of the $1/8^\circ$
197 gridded observational data (approximately 140 km^2 per grid cell). Each SWAT subbasin uses the
198 meteorology from the nearest $1/8^\circ$ grid cell. Calibration was performed at 185 different
199 streamflow sites, shown in Figure 2, where naturalized or unimpaired streamflow observations
200 were available. All SWAT models were calibrated and validated, at the 185 sites, during the
201 1950-2005 time period, though because observations were not complete at all sites some gauges
202 did not encompass the entire period. The contributing drainage areas of these sites varied from

203 approximately 100 km² to 600,000 km², and these calibration sites are the locations where
204 streamflows are analyzed for this study. The parameterization, calibration, and validation of the
205 SWAT model used in this study for three major Western United States river basins is described
206 in detail in other references (Ficklin et al., 2012;2013, 2014).

207 The streamflow metrics applied in this study are the annual 3-day peak flow and 7-day low flow
208 at each site, and only the validation period of 1990-2011 is used. These metrics aim to quantify
209 extreme high and low values without applying a theoretical distribution, as would be required to
210 estimate more rare events from the relatively short validation period. The 3-day peak flow is a
211 widely used measure for flood planning purposes (e.g., Das et al., 2013) and the 7-day low flow
212 is frequently used for characterizing water quality and ecosystem impacts (WMO, 2009). The
213 annual extreme streamflow values are analyzed using the non-parametric Mann-Whitney U test
214 (Haan, 2002) for equality of medians to determine the significance of the difference between
215 flows driven by observations and those driven by downscaled reanalysis data.

216 **3 Results and Discussion**

217 As an overview of the larger domain of the study, Figure 3 shows the biases in mean annual
218 (daily) precipitation for each of the experiments. Figure 3 demonstrates that, as will always be
219 the case due to natural variability, the biases between climate model output (or reanalyses) and
220 observations will be different for different time periods. It is also evident, for the precipitation
221 statistic depicted, that the difference in bias between the two periods is much smaller than the
222 bias itself, explaining why bias correction generally does improve skill, especially given the role
223 of topography in precipitation formation and the lack of detailed topographic representation in
224 the large-scale reanalysis data (e.g., Maurer et al., 2013). Comparing the change in bias between

225 the two periods at different spatial scales (each row of the right column), Figure 3 shows that the
226 non-stationarity has the same overall pattern at all scales, but at finer scales there is greater
227 spatial variability, with some isolated grid cells showing greater non-stationarity at fine scales.
228 Figure 3 shows the mountainous regions to have higher biases (and greater values for non-
229 stationarity), which may be expected given greater local complexity of the terrain and thus more
230 heterogeneity in the local precipitation that the bias correction is attempting to correct. However,
231 the apparent higher non-stationarity in mountainous areas is also partially due to the greater
232 precipitation at high elevations. Expressing bias as a relative change in bias (by dividing the bias
233 at each grid cell by the mean observed precipitation) shows higher non-stationarity, and the
234 amplification at some locations, to occur in some mountainous areas but also more broadly over
235 much of the domain, including some prominent valleys such as California's Central Valley. The
236 mechanisms driving the spatial variability in bias non-stationarity, and its amplification when
237 bias correcting at finer scales, is reserved for future research. These locations where non-
238 stationarity is amplified could be a concern for cases where bias correction is applied at fine
239 scales, as there would be increased risk that the bias correction could ultimately degrade the skill
240 of the climate data. A similar plot to Figure 3, but for annual maximum precipitation, showed
241 comparable patterns and characteristics.

242 To illustrate how these characteristics vary at different scales, Figure 4 shows the impact of bias
243 correction at different spatial scales on the downscaled precipitation at a single grid cell. Only
244 quantiles above 0.5 (50% non-exceedence probability) are shown to focus on the higher
245 precipitation values. While not used for quantitative analysis at this point, Figure 4 does
246 demonstrate some of the impacts of performing bias correction at different scales. As would be
247 expected, interpolating the reanalysis data to the $1/8^\circ$ spatial scale prior to bias correction

248 (employing the SDBC technique as noted above) provides the best fit to the observations for the
249 calibration period. However, Figure 4 shows that this also provides the worst correspondence to
250 the CDF for observations at most quantiles during the validation period, illustrating that the
251 instability of the biases at the finer scale may be a disincentive to performing the bias correction
252 at too fine a scale. In other words, the CDF of precipitation at the finest resolution used here
253 ($1/8^\circ$) is likely not as stationary between two time periods as a CDF at a larger spatial scale
254 would be. It should be noted that this stark of an example will not exist at every grid cell. Eden et
255 al. (2012) suggest that model errors due to unrepresented topographic effects on precipitation or
256 inadequate climate model parameterization are most successfully corrected by quantile mapping,
257 so where other small scale variability is less important there may be more successful removal of
258 biases using quantile mapping at finer scales.

259 While precipitation is the primary variable affecting streamflow, in many parts of the Western
260 United States temperature has a large impact in the hydrologic response to a changing climate,
261 due to its effect on the nature of precipitation and the rate of snowmelt (Barnett et al., 2008).
262 Figure 5 is similar to the lower panel of Figure 4, showing the CDFs (for quantiles above 0.5) for
263 the validation period for maximum and minimum daily temperatures for the same location. At
264 this one sample point performing the bias correction of minimum temperatures at the finer spatial
265 resolution provides the closest correspondence to the observations at these higher quantiles, with
266 progressively worse results with bias correction at the larger scales. For maximum temperature,
267 the results are inverted, with bias correction at the largest scale appearing slightly closer to
268 observations, though all resolutions are clustered together. This shows how the results can vary
269 across quantiles, for different variables, as well as with location (shown in Figure 3).

270 Since the interest of this study is on the ultimate hydrologic impacts of these differences in
271 downscaling approaches, not the precipitation or temperature, we turn the focus to how
272 streamflow skill is affected by bias correction at different spatial scales. Figure 6 shows the
273 distribution of daily streamflows simulated by the SWAT model for the Tule River basin (see
274 Figure 2), which has a contributing drainage area of 1,015 km², approximately equivalent to 1/3°
275 spatial resolution. The simulated flows are overpredicted at all quantiles for this location, with
276 the departure more visible at the high and low extremes. The upper right panel of Figure 6 shows
277 that for the highest 10% of daily flows performing bias correction at the coarsest 2° resolution
278 results produces less correspondence with observations than bias correcting at finer resolutions,
279 while other spatial resolutions are more tightly clustered. Only the most extreme flows (the
280 highest 1%) show a change in the spatial resolution with the higher skill, where the 0.5°
281 experiment more closely resembles the observed flow probabilities. The lower right panel in
282 Figure 6 plots the lower 10% of stream flows, showing the 2° and 1° experiments overpredicting
283 the observed flow frequency more than those at 0.5°, 0.25°, and 0.125°, which are all nearly
284 coincident.

285 As a point of contrast, Figure 7 shows the same information as Figure 6 but for a larger basin, the
286 Sacramento River (see Figure 2), which has a drainage area of 18,835 km², approximately
287 equivalent to a 1.4° spatial scale. Similar to the smaller Tule River site, the experiment with the
288 bias correction performed at 2° performed worst overall, especially evident at high flows (shown
289 in the upper right panel of Figure 7). The 1° bias correction produced the best correspondence
290 with observed flows at the low extremes (lower right panel), with the coarse 2° overpredicting
291 daily low flow magnitudes and the finer scale 0.25° and 0.125° bias correction underpredicting

292 low flows to the greatest degree. As with Figure 6, Figure 7 shows worse performance of bias
293 correction in many cases at the high and low extremes compared to the center of the distribution,
294 as would be expected with fewer observations for defining the driving precipitation and
295 temperature CDFs in the relatively short calibration period. Thus, while quantile mapping
296 generally reduces the biases compared to using raw GCM output, significant biases may remain,
297 especially at the tails of the distributions. If streamflows produced using bias corrected and
298 downscaled GCM output are to be used for analysis of extreme events, it may be desirable to use
299 a further bias correction (such as quantile mapping of simulated streamflows to match observed
300 streamflows), as has been done for water resources system operations and seasonal forecasting
301 (Snover et al., 2003; Yuan and Wood, 2012) to ensure downscaled streamflows are comparable to
302 observations at all quantiles.

303 Figures 6 and 7 raise the question of whether a limit exists for the scale at which bias correction
304 should be performed, or whether, for improved skill of simulated daily streamflows there may be
305 a correspondence between the scale at which bias correction is done and the drainage area of the
306 streamflow site. To investigate this, Figure 8 shows the results of the Mann-Whitney U test for
307 all basins for 3-day maximum flows. Since the null hypothesis is that the streamflows produced
308 by driving the SWAT model with observations are statistically indistinguishable from simulated
309 flows using downscaled Reanalysis data, a small p-value indicates that the two can be
310 confidently claimed to be different. There is no clear relationship between drainage areas and the
311 skill (defined by the p-values) for the different experiments. One observation based on Figure 8
312 is that there are more basins with p-values < 0.1 (indicating low correspondence between
313 observation- and reanalysis-driven streamflows) when bias correction is done at 2.0° than for the
314 other experiments. Regardless of the spatial scale of the bias correction, there are always some

315 small basins ($<1000 \text{ km}^2$) where the correspondence between observation- and reanalysis-driven
316 streamflows is weak. Bias correction at scales smaller than 0.5° appears to offer little
317 improvement in skill, and may even result in more streamflow sites having poor skill ($p < 0.1$).
318 This apparent 0.5° limit may reflect both the finest scale at which the large-scale reanalysis
319 variance in meteorology can be effectively rescaled (Maraun, 2013) and the degradation of
320 larger-scale spatial structure of driving meteorology (Bárdossy and Pegram, 2012) when
321 applying quantile mapping bias correction at finer spatial scales.

322 Figure 9 shows the relationship between the Mann-Whitney p-value and the drainage area for
323 each of the streamflow sites for 7-day minimum flows. Similar to the 3-day peak flows, there is a
324 weak correspondence between the scale at which the bias correction is performed and the skill
325 for basins of different drainage areas. As with 3-day peak flows, bias correction at 0.5° appears
326 as a point at which finer scale bias correction does not offer any improvement, and may increase
327 the number of streamflow sites with poor correspondence with observation-driven streamflows.
328 Table 1 summarizes the results of Figures 8 and 9, listing the number of streamflow sites for
329 which skill is low, both for $p < 0.1$ and $p < 0.05$. The bias correction being performed at 0.5° is
330 revealed as an optimum, confirming the visual interpretations of Figures 8 and 9.

331 Limitations of this study include the use of a single large-scale forcing data set; GCMs at
332 different native spatial resolutions may produce different results. The biases in different GCMs
333 will also affect the performance of the bias correction, and thus would affect the outcomes. The
334 spatial scale of the hydrological model, and its representation of sub-grid spatial variability, may
335 also affect the results, thus different parameterizations of the SWAT model or the use of other
336 hydrology models would affect results (Ficklin and Barnhart, 2014;Maurer et al., 2010a). Results

337 may also be dependent on the metric used for testing correspondence, for example, examining
338 impacts other than streamflow. Also, this study focused on biases at different scales for output
339 from the BCSD process as it is typically applied. We did not assess the influence of each step in
340 the BCSD process (as shown in Figure 1) on the biases, though this could be a fruitful avenue for
341 future research.

342 **4 Conclusions**

343 When applying statistical downscaling methods to adapt climate model data for use in regional
344 hydrologic impacts studies, a bias correction step is typically included. A common method for
345 bias correction is quantile mapping, which can be performed in many different ways. One way in
346 which applications of quantile mapping vary is in the spatial scale at which it is applied, which
347 can range from the large scale of climate model output (generally 1° to 4° latitude-longitude)
348 down to the finest resolution of observed data. This experiment investigated the effect of the
349 spatial scale at which precipitation (and temperature) are bias corrected (as part of a statistical
350 downscaling approach) on the streamflow produced by a hydrologic model.

351 Similar to many prior studies, as a surrogate for climate model data, this experiment used
352 reanalysis data, which is at a spatial scale of approximately 1.9°. A gridded observational dataset
353 of daily precipitation and temperature was used as the observational baseline, and was
354 aggregated to spatial resolutions of 0.125°, 0.25°, 0.5°, 1.0° and 2.0° to be used in the bias
355 correction step of the statistical downscaling scheme. The principal findings were that bias
356 correction at the coarsest scale (2.0°) performed worst, and performing bias correction at scales
357 finer than 0.5° produced little additional benefit, and even degraded the correspondence between
358 observation-driven streamflows and those driven by downscaled meteorology.

359 This suggests that the primary assumption inherent in quantile mapping bias correction, namely
360 that the biases between modeled and observed meteorological variables for a calibration period
361 are relatively stationary in time and can be applied to a projected period, may become less valid
362 at spatial resolution finer than approximately 0.5° . This may indicate a shift in the sources of
363 uncertainty causing the biases as spatial resolution changes. Some biases, such as those caused
364 by inadequate topographic representation in the large-scale model, are better described at fine
365 scales and benefit from having bias correction performed at as fine a scale as possible. Other
366 biases, due to incorrect location of climate features at the larger scale, may be less able to be
367 corrected at very fine spatial scales (e.g., Maraun and Widmann, 2015). For the region and data
368 sources used in this study, the spatial resolution of 0.5° , or approximately a 50 km scale, appears
369 to provide an optimal balance between these competing effects.

370 The findings of this study caution against the temptation to apply quantile mapping bias
371 correction at the finest possible scale, even though it provides the closest correspondence to
372 observations for the calibration period. For independent validation periods, these findings
373 suggest that very fine scale quantile mapping will perform no better, and possibly worse, than
374 coarsening observations to approximately 0.5° , and applying bias correction at that scale.

375

376

377 **Acknowledgements**

378 This work was supported by NASA Earth Exchange (NEX, www.nex.nasa.gov) at NASA Ames
379 Research Center and the Bay Area Environmental Research Institute.

380 **Author contribution:** E.P.M. designed the experiment and performed the downscaling. D.L.F.
381 conducted hydrologic modeling. W.W. provided interpretation of results. E.P.M. prepared the
382 manuscript with contributions from all co-authors.

383

384 **References**

- 385 Abatzoglou, J. T., and Brown, T. J.: A comparison of statistical downscaling methods suited for wildfire
386 applications, *Int. J. Climatol.*, 32, 772-780, 10.1002/joc.2312, 2012.
- 387 Arnold, J. G., Srinivasan, R., Muttiah, R. S., and Williams, J. R.: Large Area Hydrologic Modeling and
388 Assessment Part I: Model Development, *JAWRA Journal of the American Water Resources
389 Association*, 34, 73-89, 10.1111/j.1752-1688.1998.tb05961.x, 1998.
- 390 Bárdossy, A., and Pegram, G.: Multiscale spatial recorelation of RCM precipitation to produce unbiased
391 climate change scenarios over large areas and small, *Water Resour. Res.*, 48, W09502,
392 10.1029/2011wr011524, 2012.
- 393 Barnett, T. P., Pierce, D. W., Hidalgo, H. G., Bonfils, C., Santer, B. D., Das, T., Bala, G., Wood, A. W.,
394 Nozawa, T., Mirin, A. A., Cayan, D. R., and Dettinger, M. D.: Human-Induced Changes in the
395 Hydrology of the Western United States, *Science*, 319, 1080-1083,
396 doi:10.1126/science.1152538, 10.1126/science.1152538, 2008.
- 397 Das, T., Maurer, E. P., Pierce, D. W., Dettinger, M. D., and Cayan, D. R.: Increases in flood magnitudes in
398 California under warming climates, *J. Hydrol.*, 501, 101-110,
399 <http://dx.doi.org/10.1016/j.jhydrol.2013.07.042>, 2013.
- 400 Eden, J. M., Widmann, M., Grawe, D., and Rast, S.: Skill, Correction, and Downscaling of GCM-Simulated
401 Precipitation, *J. Climate*, 25, 3970-3984, 10.1175/jcli-d-11-00254.1, 2012.
- 402 Ehret, U., Zehe, E., Wulfmeyer, V., Warrach-Sagi, K., and Liebert, J.: HESS Opinions "Should we apply bias
403 correction to global and regional climate model data?", *Hydrol. Earth Syst. Sci.*, 16, 3391-3404,
404 doi:3310.5194/hess-3316-3391-2012, 2012.
- 405 Ficklin, D. L., Stewart, I. T., and Maurer, E. P.: Projections of 21st Century Sierra Nevada Local Hydrologic
406 Flow Components Using an Ensemble of General Circulation Models1, *JAWRA Journal of the
407 American Water Resources Association*, 48, 1104-1125, 10.1111/j.1752-1688.2012.00675.x,
408 2012.
- 409 Ficklin, D. L., Stewart, I. T., and Maurer, E. P.: Climate Change Impacts on Streamflow and Subbasin-Scale
410 Hydrology in the Upper Colorado River Basin, *PLoS ONE*, 8, e71297.
411 doi:71210.71371/journal.pone.0071297, 2013.
- 412 Ficklin, D. L., and Barnhart, B. L.: SWAT hydrologic model parameter uncertainty and its implications for
413 hydroclimatic projections in snowmelt-dependent watersheds, *J. Hydrol.*, 519, Part B, 2081-
414 2090, <http://dx.doi.org/10.1016/j.jhydrol.2014.09.082>, 2014.
- 415 Ficklin, D. L., Barnhart, B. L., Knouft, J. H., Stewart, I. T., Maurer, E. P., Letsinger, S. L., and Whittaker, G.
416 W.: Climate change and stream temperature projections in the Columbia River basin: habitat
417 implications of spatial variation in hydrologic drivers, *Hydrol. Earth Syst. Sci.*, 18, 4897-4912,
418 10.5194/hess-18-4897-2014, 2014.
- 419 Flato, G., Marotzke, J., Abiodun, B., Braconnot, P., Chou, S. C., Collins, W., Cox, P., Driouech, F., Emori, S.,
420 Eyring, V., Forest, C., Gleckler, P., Guilyardi, E., Jakob, C., Kattsov, V., Reason, C., and
421 Rummukainen, M.: Evaluation of Climate Models, in: *Climate Change 2013: The Physical Science
422 Basis. Contribution of Working Group I to the Fifth Assessment Report of the Intergovernmental
423 Panel on Climate Change*, edited by: Stocker, T. F., Qin, D., Plattner, G.-K., Tignor, M., Allen, S. K.,
424 Boschung, J., Nauels, A., Xia, Y., Bex, V., and Midgley, P. M., Cambridge University Press,
425 Cambridge, United Kingdom and New York, NY, USA, 741-866, 2013.
- 426 Gudmundsson, L., Bremnes, J. B., Haugen, J. E., and Engen-Skaugen, T.: Technical Note: Downscaling
427 RCM precipitation to the station scale using statistical transformations - a comparison of
428 methods, *Hydrol. Earth Syst. Sci.*, 16, 3383-3390, 10.5194/hess-16-3383-2012, 2012.

429 Haan, C. T.: Statistical Methods in Hydrology, second edition, Iowa State Press, Ames, IA, USA, 496 pp.,
430 2002.

431 Haerter, J. O., Eggert, B., Moseley, C., Piani, C., and Berg, P.: Statistical precipitation bias correction of
432 gridded model data using point measurements, *Geophys. Res. Lett.*, 42, 1919-1929,
433 10.1002/2015gl063188, 2015.

434 Hawkins, E., and Sutton, R.: The Potential to Narrow Uncertainty in Regional Climate Predictions, *Bull.*
435 *Am. Met. Soc.*, 90, 1095-1107, 10.1175/2009BAMS2607.1, 2009.

436 Hawkins, E., and Sutton, R.: The potential to narrow uncertainty in projections of regional precipitation
437 change, *Clim. Dyn.*, 37, 407-418, 10.1007/s00382-010-0810-6, 2011.

438 Huth, R.: Statistical downscaling of daily temperature in Central Europe, *J. Climate*, 15, 1731-1742, 2002.

439 Hwang, S., and Graham, W. D.: Development and comparative evaluation of a stochastic analog method
440 to downscale daily GCM precipitation, *Hydrol. Earth Syst. Sci.*, 17, 4481-4502, 10.5194/hess-17-
441 4481-2013, 2013.

442 Kalnay, E., Kanamitsu, M., Kistler, R., Collins, W., Deaven, D., Gandin, L., Iredell, M., Saha, S., White, G.,
443 Woollen, J., Zhu, Y., Leetmaa, A., and Reynolds, B.: The NCEP/NCAR 40-year reanalysis project,
444 *Bull. Am. Met. Soc.*, 77, 437-472, 1996.

445 Lafon, T., Dadson, S., Buys, G., and Prudhomme, C.: Bias correction of daily precipitation simulated by a
446 regional climate model: a comparison of methods, *Int. J. Climatol.*, 1-15, doi: 10.1002/joc.3518,
447 10.1002/joc.3518, 2012.

448 Li, H., Sheffield, J., and Wood, E. F.: Bias correction of monthly precipitation and temperature fields from
449 Intergovernmental Panel on Climate Change AR4 models using equidistant quantile matching, *J.*
450 *Geophys. Res.*, 115, D10101, 10.1029/2009jd012882, 2010.

451 Li, J., Sharma, A., Johnson, F., and Evans, J.: Evaluating the effect of climate change on areal reduction
452 factors using regional climate model projections, *J. Hydrol.*, 528, 419-434,
453 <http://dx.doi.org/10.1016/j.jhydrol.2015.06.067>, 2015.

454 Livneh, B., Rosenberg, E. A., Lin, C., Nijssen, B., Mishra, V., Andreadis, K. M., Maurer, E. P., and
455 Lettenmaier, D. P.: A Long-Term Hydrologically Based Dataset of Land Surface Fluxes and States
456 for the Conterminous United States: Update and Extensions*, *J. Climate*, 26, 9384-9392,
457 10.1175/jcli-d-12-00508.1, 2013.

458 Maraun, D., Wetterhall, F., Ireson, A. M., Chandler, R. E., Kendon, E. J., Widmann, M., Brienen, S., Rust,
459 H. W., Sauter, T., Themeßl, M., Venema, V. K. C., Chun, K. P., Goodess, C. M., Jones, R. G., Onof,
460 C., Vrac, M., and Thiele-Eich, I.: Precipitation downscaling under climate change: Recent
461 developments to bridge the gap between dynamical models and the end user, *Rev. Geophys.*,
462 48, RG3003, 10.1029/2009rg000314, 2010.

463 Maraun, D.: Nonstationarities of regional climate model biases in European seasonal mean temperature
464 and precipitation sums, *Geophys. Res. Lett.*, 39, L06706, 10.1029/2012gl051210, 2012.

465 Maraun, D.: Bias Correction, Quantile Mapping, and Downscaling: Revisiting the Inflation Issue, *J.*
466 *Climate*, 26, 2137-2143, 10.1175/jcli-d-12-00821.1, 2013.

467 Maraun, D.: Reply to "Comment on 'Bias Correction, Quantile Mapping, and Downscaling: Revisiting the
468 Inflation Issue'", *J. Climate*, 27, 1821-1825, 10.1175/jcli-d-13-00307.1, 2014.

469 Maraun, D., and Widmann, M.: The representation of location by regional climate models in complex
470 terrain, *Hydrol. Earth Syst. Sci. Discuss.*, 12, 3011-3028, 10.5194/hessd-12-3011-2015, 2015.

471 Maurer, E. P., O'Donnell, G. M., Lettenmaier, D. P., and Roads, J. O.: Evaluation of the land surface water
472 budget in NCEP/NCAR and NCEP/DOE reanalyses using an off-line hydrologic model, *J. Geophys*
473 *Res.*, 106, 17841-17862, 2001.

474 Maurer, E. P., Brekke, L. D., Pruitt, T., and Duffy, P. B.: Fine-resolution climate change projections
475 enhance regional climate change impact studies, *Eos Trans. AGU*, 88, 504,
476 doi:510.1029/2007EO470006, 2007.

477 Maurer, E. P., Brekke, L. D., and Pruitt, T.: Contrasting Lumped and Distributed Hydrology Models for
478 Estimating Climate Change Impacts on California Watersheds¹, *JAWRA Journal of the American*
479 *Water Resources Association*, 46, 1024-1035, 10.1111/j.1752-1688.2010.00473.x, 2010a.

480 Maurer, E. P., Hidalgo, H. G., Das, T., Dettinger, M. D., and Cayan, D. R.: The utility of daily large-scale
481 climate data in the assessment of climate change impacts on daily streamflow in California,
482 *Hydrol. Earth System Sci.*, 14, 1125-1138, doi:110.5194/hess-1114-1125-2010, 2010b.

483 Maurer, E. P., Das, T., and Cayan, D. R.: Errors in climate model daily precipitation and temperature
484 output: time invariance and implications for bias correction, *Hydrol. Earth Syst. Sci.*, 17, 2147-
485 2159, 10.5194/hess-17-2147-2013, 2013.

486 Maurer, E. P., Brekke, L., Pruitt, T., Thrasher, B., Long, J., Duffy, P., Dettinger, M., Cayan, D., and Arnold,
487 J.: An enhanced archive facilitating climate impacts and adaptation analysis, *Bull. Am. Met. Soc.*,
488 10.1175/bams-d-13-00126.1, 2014.

489 Meehl, G. A., Covey, C., Delworth, T., Latif, M., McAvaney, B., Mitchell, J. F. B., Stouffer, R. J., and Taylor,
490 K. E.: The WCRP CMIP3 multimodel dataset: A new era in climate change research, *Bull. Am.*
491 *Met. Soc.*, 88, 1383-1394, 2007.

492 Mehrotra, R., and Sharma, A.: An improved standardization procedure to remove systematic low
493 frequency variability biases in GCM simulations, *Water Resour. Res.*, 48, W12601,
494 10.1029/2012WR012446, 2012.

495 Mehrotra, R., and Sharma, A.: Correcting for systematic biases in multiple raw GCM variables across a
496 range of timescales, *J. Hydrol.*, 520, 214-223, <http://dx.doi.org/10.1016/j.jhydrol.2014.11.037>,
497 2015.

498 Panofsky, H. A., and Brier, G. W.: *Some Applications of Statistics to Meteorology*, The Pennsylvania State
499 University, University Park, PA, USA, 224 pp., 1968.

500 Piani, C., Haerter, J., and Coppola, E.: Statistical bias correction for daily precipitation in regional climate
501 models over Europe, *Theor. Appl. Climatol.*, 99, 187-192, 10.1007/s00704-009-0134-9, 2010.

502 Pierce, D. W., Cayan, D. R., Maurer, E. P., Abatzoglou, J. T., and Hegewisch, K. C.: Improved Bias
503 Correction Techniques for Hydrological Simulations of Climate Change, *J. Hydrometeorology*, 16,
504 2421-2442, 10.1175/JHM-D-14-0236.1, 2015.

505 Reichler, T., and Kim, J.: How Well Do Coupled Models Simulate Today's Climate?, *Bull. Am. Met. Soc.*,
506 89, 303-311, doi:310.1175/BAMS-1189-1173-1303, 2008.

507 Schmidli, J., Frei, C., and Vidale, P. L.: Downscaling from GCM precipitation: A benchmark for dynamical
508 and statistical downscaling, *Int. J. Climatol.*, 26, 679-689, 2006.

509 Sheffield, J., Barrett, A., Colle, B., Fernando, D. N., Fu, R., Geil, K. L., Hu, Q., Kinter, J., Kumar, S.,
510 Langenbrunner, B., Lombardo, K., Long, L. N., Maloney, E., Mariotti, A., Meyerson, J. E., Mo, K.
511 C., Neelin, J. D., Nigam, S., Pan, Z., Ren, T., Ruiz-Barradas, A., Serra, Y. L., Seth, A., Thibeault, J.
512 M., Stroeve, J. C., Yang, Z., and Yin, L.: North American Climate in CMIP5 Experiments. Part I:
513 Evaluation of Historical Simulations of Continental and Regional Climatology, *J. Climate*,
514 10.1175/jcli-d-12-00592.1, 2013a.

515 Sheffield, J., Langenbrunner, B., Meyerson, J. E., Neelin, J. D., Camargo, S. J., Fu, R., Hu, Q., Jiang, X.,
516 Karnauskas, K. B., Kim, S. T., Kumar, S., Kinter, J., Maloney, E. D., Mariotti, A., Pan, Z., Ruiz-
517 Barradas, A., Nigam, S., Seager, R., Serra, Y. L., Sun, D.-Z., Wang, C., Yu, J.-Y., Johnson, N., Xie, S.-
518 P., Zhang, T., and Zhao, M.: North American Climate in CMIP5 Experiments. Part II: Evaluation of
519 Historical Simulations of Intra-Seasonal to Decadal Variability, *J. Climate*, 10.1175/jcli-d-12-
520 00593.1, 2013b.

521 Snover, A. K., Hamlet, A. F., and Lettenmaier, D. P.: Climate-Change Scenarios for Water Planning
522 Studies: Pilot Applications in the Pacific Northwest, *Bull. Am. Met. Soc.*, 84, 1513-1518,
523 10.1175/BAMS-84-11-1513, 2003.

524 Taylor, K. E., Stouffer, R. J., and Meehl, G. A.: An Overview of CMIP5 and the experiment design, *Bull.*
525 *Am. Met. Soc.*, 93, 485-498, doi:10.1175/BAMS-D-1111-00094.00091, 2012.

526 Teutschbein, C., and Seibert, J.: Is bias correction of regional climate model (RCM) simulations possible
527 for non-stationary conditions?, *Hydrol. Earth Syst. Sci.*, 17, 5061-5077, 10.5194/hess-17-5061-
528 2013, 2013.

529 Themeßl, M., Gobiet, A., and Leuprecht, A.: Empirical-statistical downscaling and error correction of
530 daily precipitation from regional climate models, *Int. J. Climatol.*, 31, 1530-1544,
531 10.1002/joc.2168, 2011.

532 Thrasher, B., Maurer, E. P., McKellar, C., and Duffy, P. B.: Technical Note: Bias correcting climate model
533 simulated daily temperature extremes with quantile mapping, *Hydrol. Earth Syst. Sci.*, 16, 3309-
534 3314, doi:10.5194/hess-3316-3309-2012, 2012.

535 Tian, D., Martinez, C. J., and Graham, W. D.: Seasonal Prediction of Regional Reference
536 Evapotranspiration Based on Climate Forecast System Version 2, *J. Hydrometeorology*, 15, 1166-
537 1188, 10.1175/jhm-d-13-087.1, 2014.

538 Tryhorn, L., and DeGaetano, A.: A comparison of techniques for downscaling extreme precipitation over
539 the Northeastern United States, *Int. J. Climatol.*, 31, 1975-1989, 10.1002/joc.2208, 2011.

540 Vrac, M., Stein, M., and Hayhoe, K.: Statistical downscaling of precipitation through nonhomogeneous
541 stochastic weather typing, *Clim. Res.*, 34, 169-184, 10.3354/cr00696, 2007.

542 Watterson, I. G., Bathols, J., and Heady, C.: What Influences the Skill of Climate Models over the
543 Continents?, *Bull. Am. Met. Soc.*, 95, 689-700, 10.1175/bams-d-12-00136.1, 2014.

544 Widmann, M., and Bretherton, C. S.: Validation of mesoscale precipitation in the NCEP reanalysis using a
545 new grid-cell precipitation dataset for the Northwestern United States, *J. Climate*, 13, 1936-
546 1950, 2000.

547 Wilby, R. L., Hay, L. E., Gutowski, W. J., Arritt, R. W., Takle, E. S., Pan, Z., Leavesley, G. H., and Clark, M.
548 P.: Hydrological responses to dynamically and statistically downscaled climate model output,
549 *Geophys. Res. Lett.*, 27, 1199-1202, 2000.

550 WMO: Manual on Low-flow Estimation and Prediction, Operational Hydrology Report No. 50, World
551 Meteorological Organization, Geneva, Switzerland, 138, 2009.

552 Wood, A. W., Leung, L. R., Sridhar, V., and Lettenmaier, D. P.: Hydrologic implications of dynamical and
553 statistical approaches to downscaling climate model outputs, *Climatic Change*, 62, 189-216,
554 2004.

555 Yuan, X., and Wood, E. F.: Downscaling precipitation or bias-correcting streamflow? Some implications
556 for coupled general circulation model (CGCM)-based ensemble seasonal hydrologic forecast,
557 *Water Resour. Res.*, 48, W12519, 10.1029/2012WR012256, 2012.

558 Zhang, F., and Georgakakos, A.: Joint variable spatial downscaling, *Climatic Change*, 111, 945-972,
559 10.1007/s10584-011-0167-9, 2012.

560

561

Table 1 - Summary of the percentage of streamflow sites with $p < 0.1$ and $p < 0.05$

562

(shown in Figures 8 and 9)

Spatial resolution used for bias-correction	Percent of sites with $p < 0.1$		Percent of sites with $p < 0.05$	
	3-day maximum flows	7-day minimum flows	3-day maximum flows	7-day minimum flows
2.0°	22.0	30.6	17.7	23.7
1.0°	12.4	19.9	5.9	14.5
0.5°	6.5	13.5	4.3	8.1
0.25°	9.1	17.2	4.3	10.8
0.125°	9.1	18.3	5.4	15.1

563

564 **List of Figures**

565 Figure 1 - Schematic of Bias Correction - Spatial Disaggregation process used in this experiment. Values
566 for X vary from 2° (latitude-longitude) to 0.125° as described in the text.

567 Figure 2 - Streamflow locations used in this study.

568 Figure 3 - Mean precipitation bias, measured as the difference between reanalysis and observations for the
569 calibration (1960-1989) and validation (1990-2011) periods, and the difference in bias between the two
570 periods. Reanalysis data are interpolated and observations aggregated to the spatial resolution indicated in
571 the left column.

572 Figure 4 - Cumulative distribution function plots (for quantiles 0.5-0.99) of bias-corrected and spatially
573 disaggregated daily precipitation for a single grid cell at latitude 45, longitude -116. Spatial resolution in
574 degrees at which the bias correction is performed is indicated in the legend. "Obs" is the CDF for the
575 observations at $1/8$ degree spatial resolution.

576 Figure 5 - Similar to Figure 4, but for the validation period for minimum daily temperature (upper panel)
577 and maximum daily temperature (lower panel).

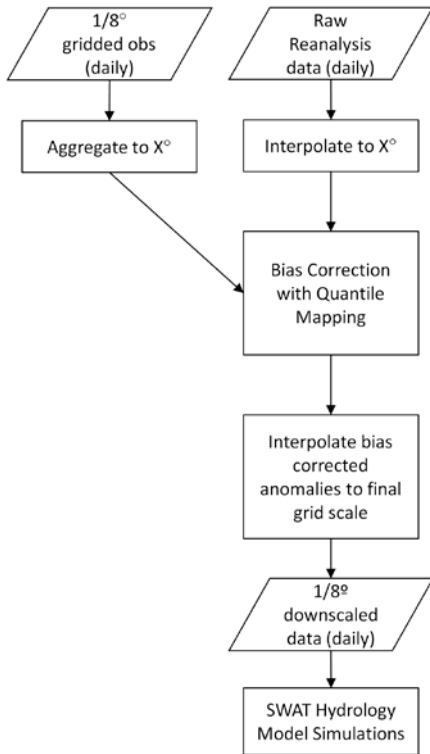
578 Figure 6 - Cumulative distribution function for the daily streamflows at the Tule River gauge. The full
579 CDF is in left panel, upper right panel expands the highest 10% of flows, and the lower right highlights
580 the 10% lowest flows.

581 Figure 7 - Similar to Figure 6, but for the Sacramento River stream gauge site.

582 Figure 8 - P-values from the Mann-Whitney U test vs. the drainage area for each of the streamflow sites
583 in Figure 2. The dashed horizontal line at $p=0.1$ is shown for reference; p-values less than this are
584 indicative of poor correspondence between observation- and reanalysis-driven streamflows.

585 Figure 9 - Similar to Figure 8, but for the 7-day low flows at each streamflow site.

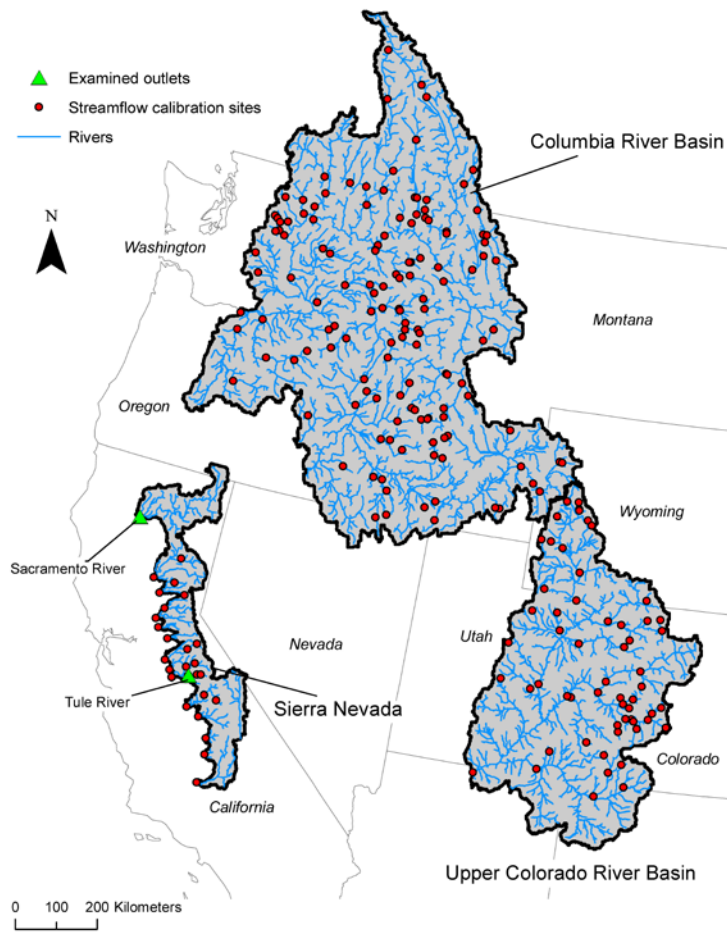
586



587

588 **Figure 1 - Schematic of Bias Correction - Spatial Disaggregation process used in this**
 589 **experiment. Values for X vary from 2° (latitude-longitude) to 0.125° as described in the**
 590 **text.**

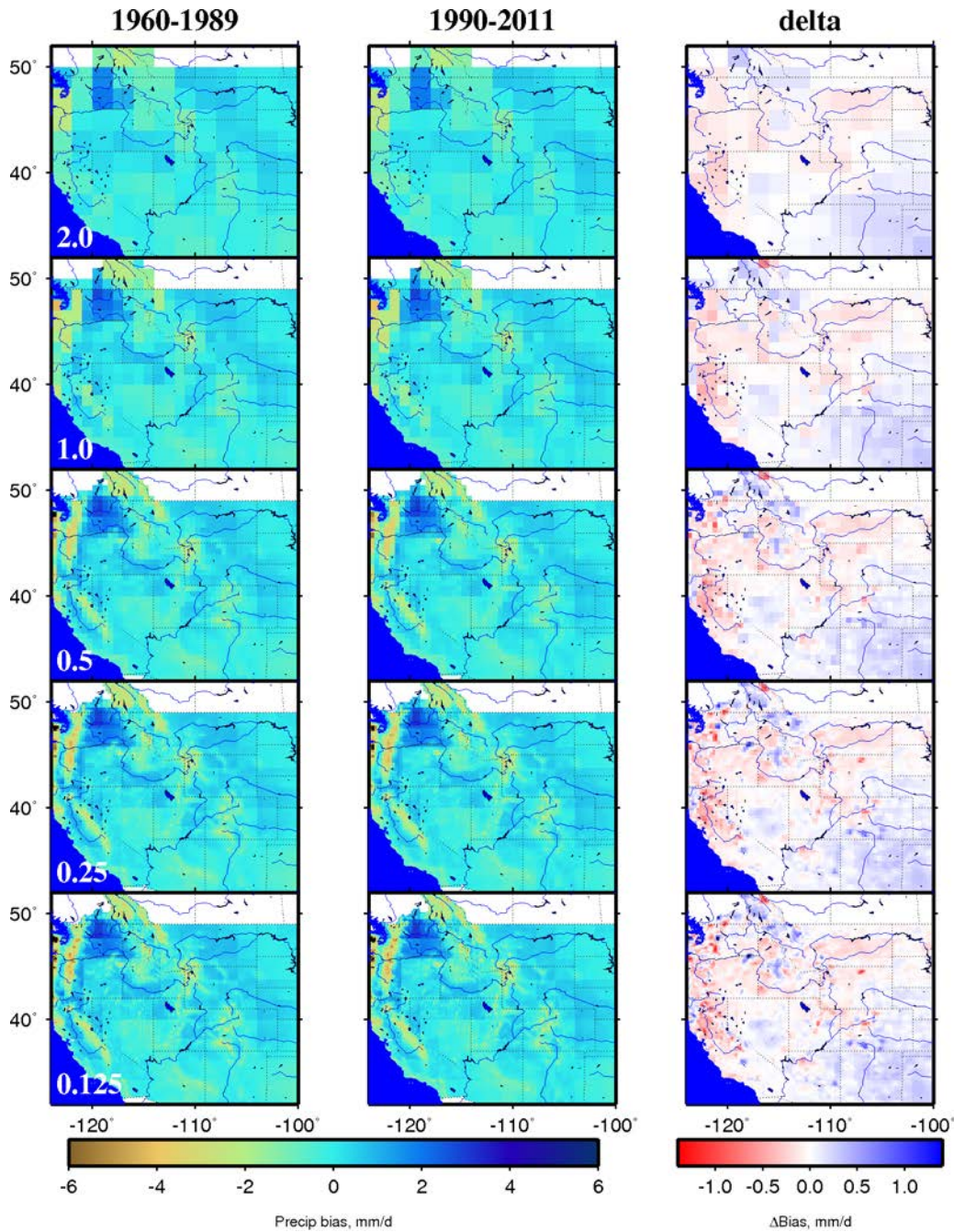
591



592

593 **Figure 2 - Streamflow locations used in this study.**

594



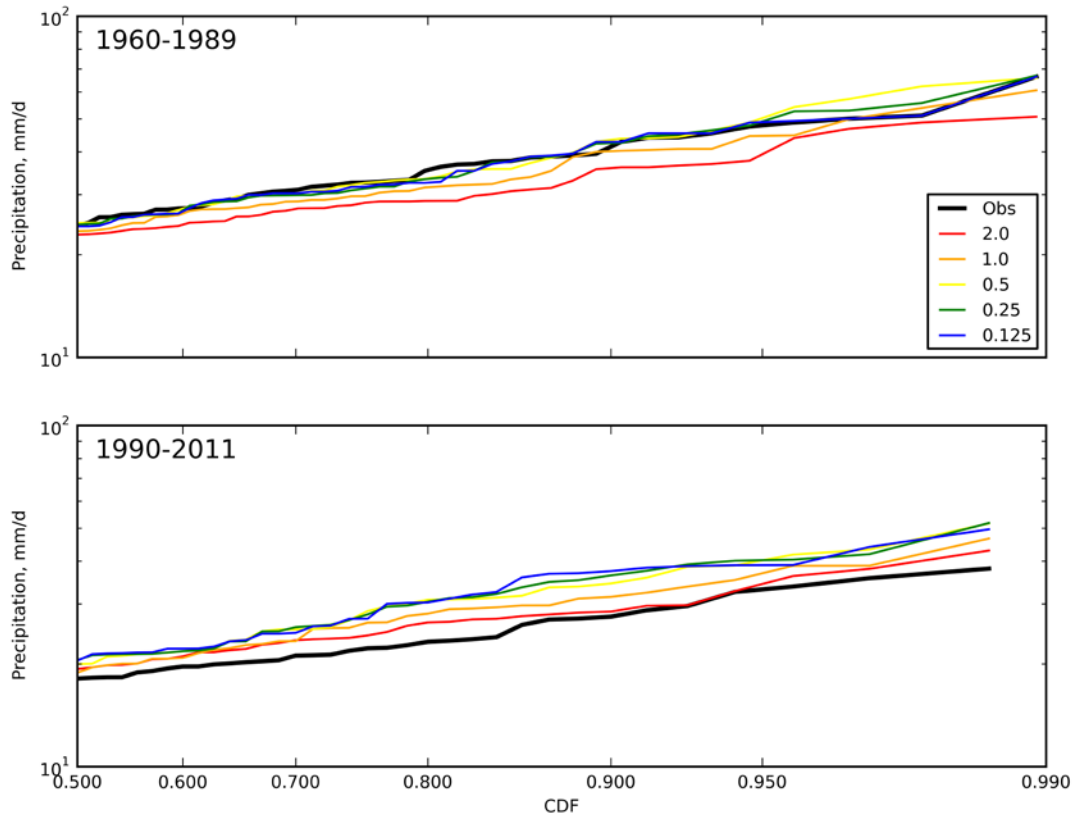
595

596 **Figure 3 - Mean precipitation bias, measured as the difference between reanalysis and**
 597 **observations for the calibration (1960-1989) and validation (1990-2011) periods, and the**
 598 **difference in bias between the two periods. Reanalysis data are interpolated and**
 599 **observations aggregated to the spatial resolution indicated in the left column.**

600

601

602

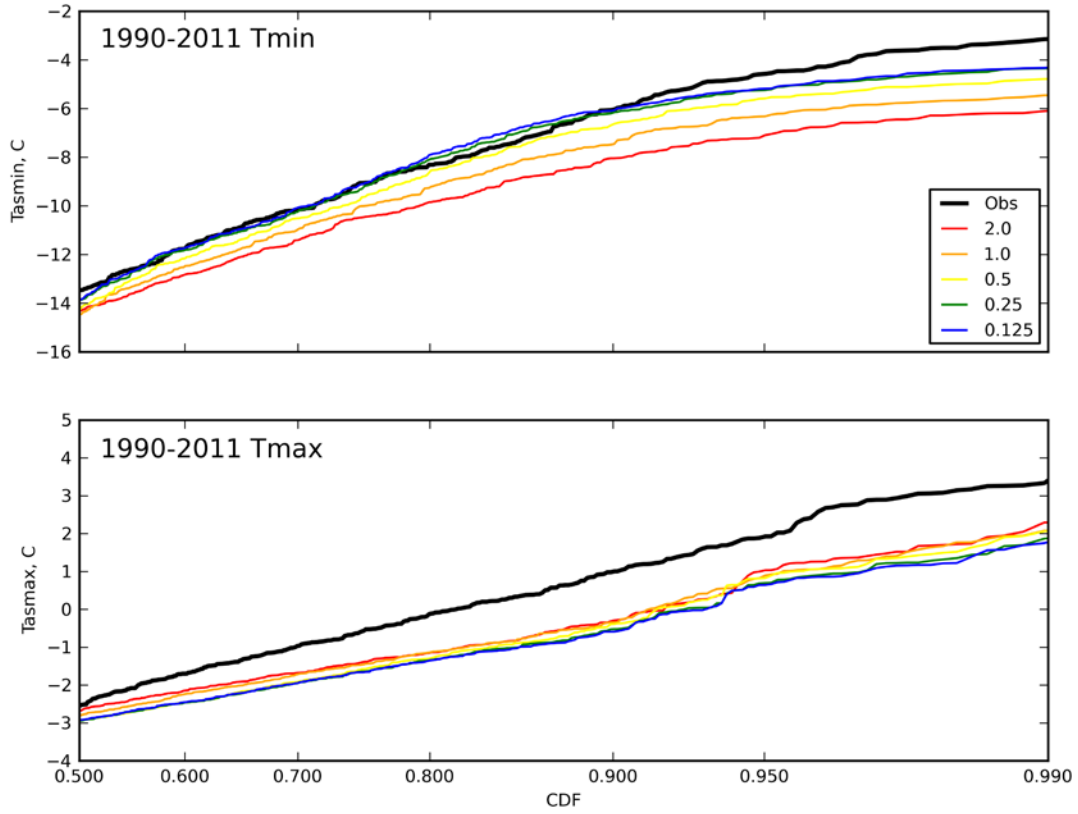


603

604 **Figure 4 - Cumulative distribution function plots (for quantiles 0.5-0.99) of bias-corrected**
605 **and spatially disaggregated daily precipitation for a single grid cell at latitude 45, longitude**
606 **-116. Spatial resolution in degrees at which the bias correction is performed is indicated in**
607 **the legend. "Obs" is the CDF for the observations at 1/8 degree spatial resolution.**

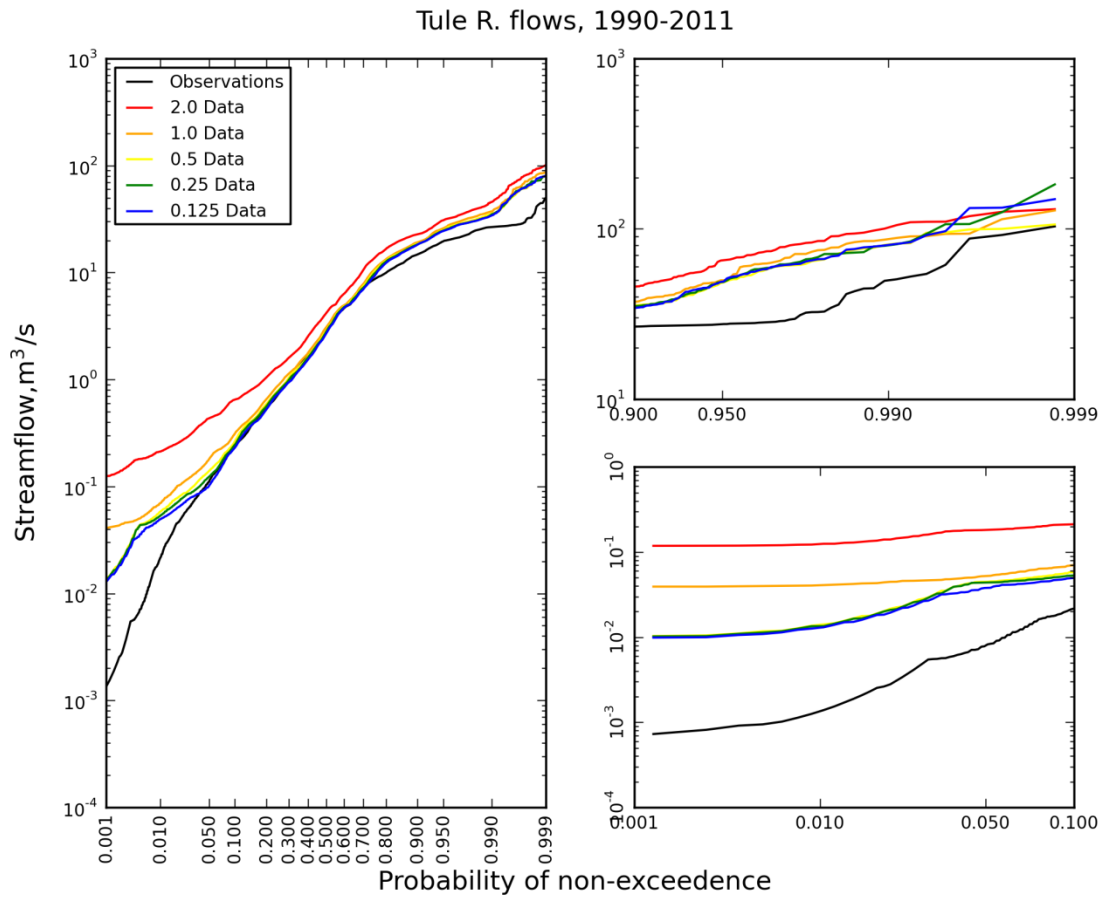
608

609



610

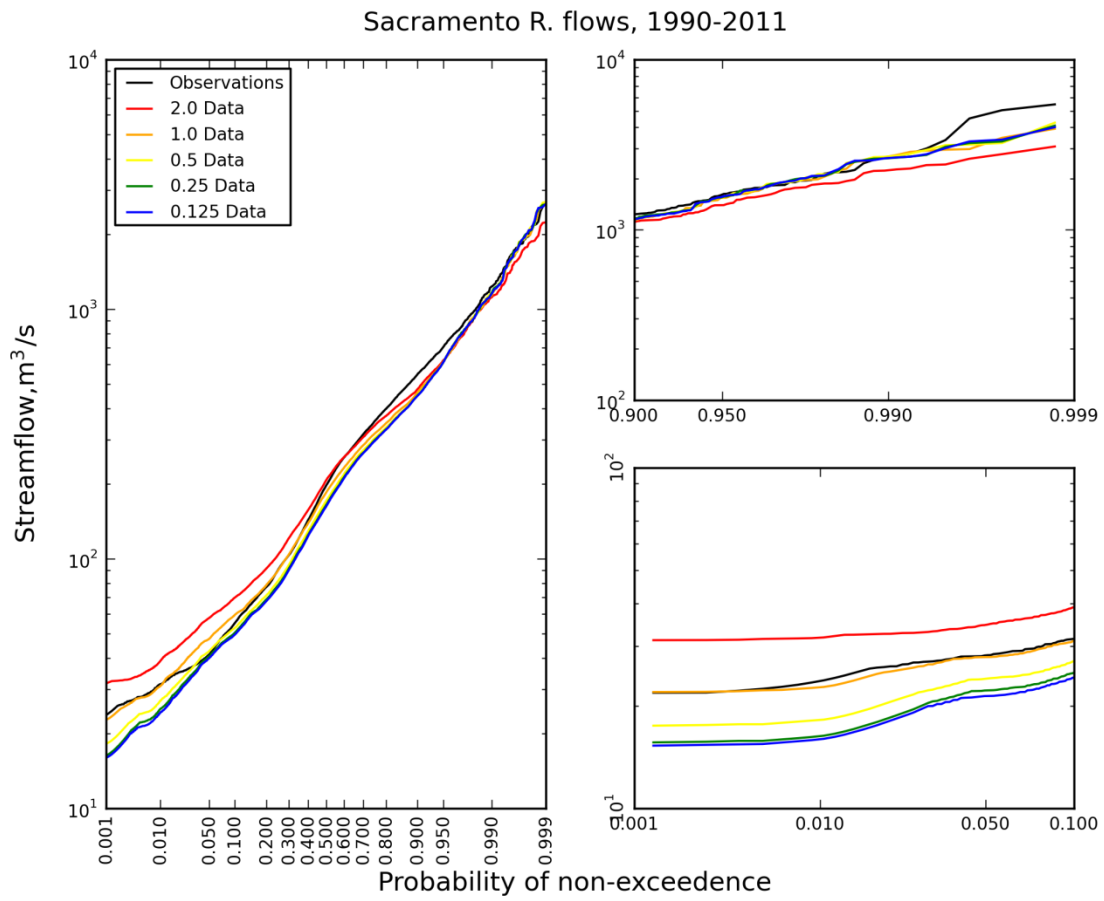
611 **Figure 5 - Similar to Figure 4, but for the validation period for minimum daily temperature**
612 **(upper panel) and maximum daily temperature (lower panel).**



613

614 **Figure 6 - Cumulative distribution function for the daily streamflows at the Tule River**
 615 **gauge. The full CDF is in left panel, upper right panel expands the highest 10% of flows,**
 616 **and the lower right highlights the 10% lowest flows.**

617

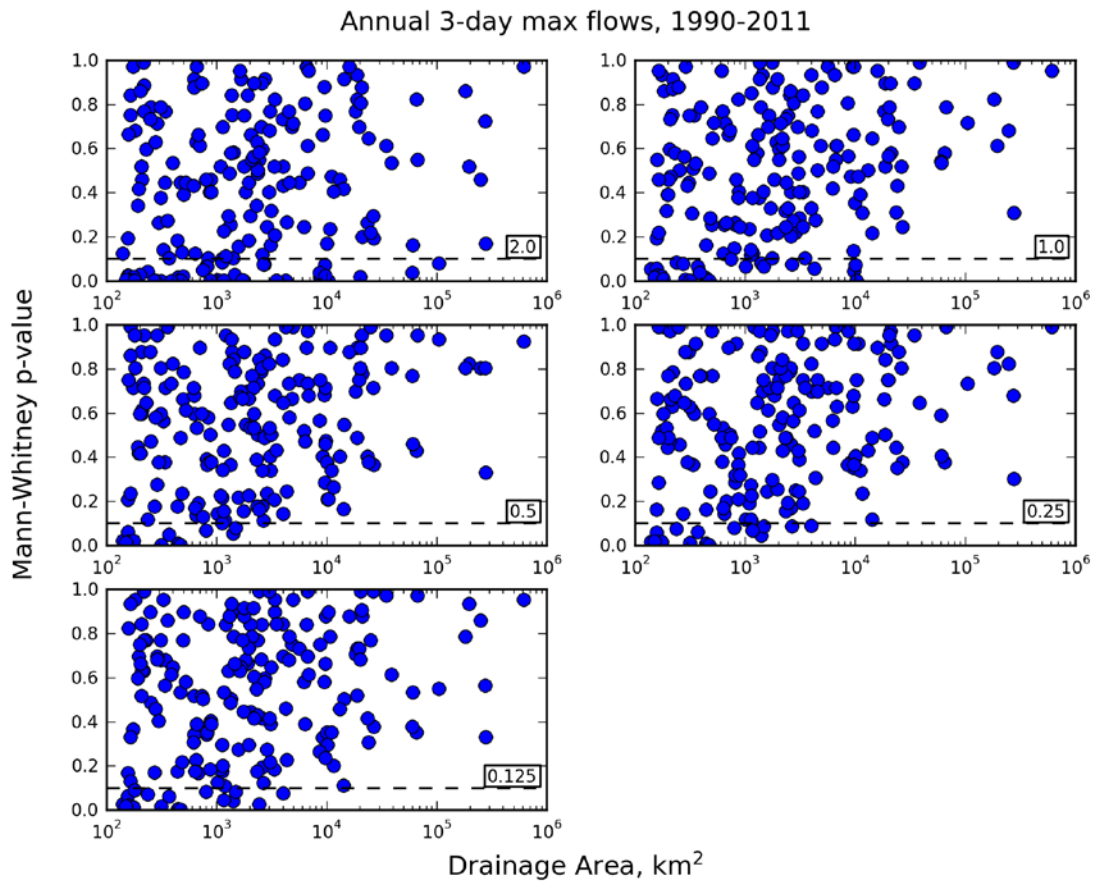


619

620 **Figure 7 - Similar to Figure 6, but for the Sacramento River stream gauge site.**

621

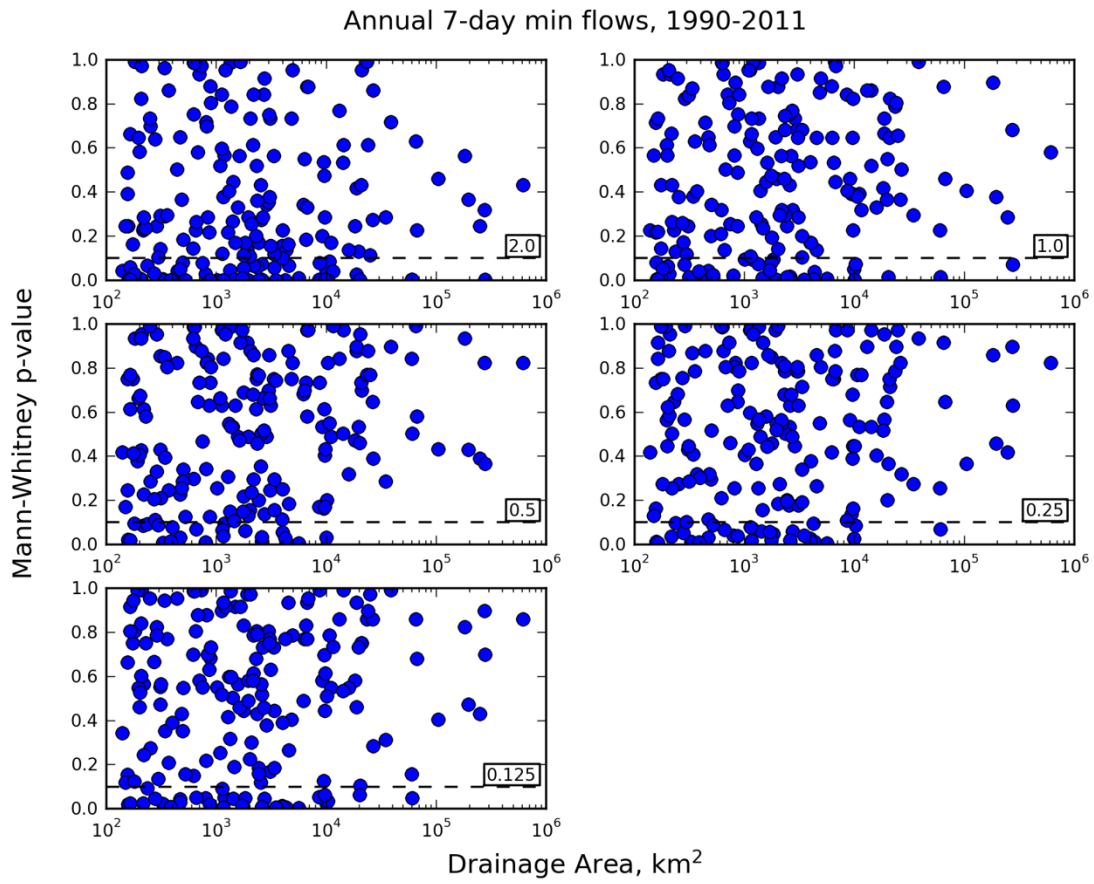
622



623

624 **Figure 8 - P-values from the Mann-Whitney U test vs. the drainage area for each of the**
625 **streamflow sites in Figure 2. The dashed horizontal line at $p=0.1$ is shown for reference; p-**
626 **values less than this are indicative of poor correspondence between observation- and**
627 **reanalysis-driven streamflows.**

628



630

631 **Figure 9 - Similar to Figure 8, but for the 7-day low flows at each streamflow site.**

632